



TECHNICAL ARTICLE

Solid-State Diffusion Bonding of Pseudo- α -Ti Alloy to Ti-Stabilized Stainless Steel: With and Without Interlayer

Harish Kumar, Sujay Bhattacharya, and Nachiket A. Keskar

Submitted: 14 January 2022 / Revised: 22 January 2022 / Accepted: 29 January 2022 / Published online: 9 March 2022

Solid-state diffusion bonding of pseudo- α -Ti alloy and Ti-stabilized stainless steel (SS321), with and without Ni interlayer, was investigated in the temperature range of 800–940 °C for different times. Microstructural investigation of the bond interfaces in the directly bonded diffusion couple showed a distinct diffusion zone which was composed of layers of (1) Fe-Ti intermetallic phases (Fe_2Ti and FeTi), (2) transformed β -Ti and (3) ($\alpha+\beta$) Ti. Shear strength of the joint was seen to be dependent on the thickness of diffusion zone and intermetallic phase layer. For direct diffusion bonding, maximum shear strength of 223.6 ± 17 MPa was observed for the joints processed at a temperature of 920 °C with a holding time of 8 min under a load corresponding to ~ 0.8 times yield strength (YS) of Ti alloy. Shear strength results showed that the optimum thickness of the Fe-Ti intermetallic phase layer is approximately 2 ± 0.5 μm . For the diffusion bonding joints in the presence of a Ni interlayer, formation of layers of Ni-Ti intermetallic compounds (Ni_3Ti , NiTi and NiTi_2) was observed at the interface between Ni and Ti alloys. Joint bonded at 940 °C with a holding time of 1 min under a load of $0.8 \times \text{YS}$ showed the maximum shear strength of 180 ± 23 MPa. The optimum thickness of the Ni-Ti intermetallic layers for maximum shear strength was found to be approximately 5 ± 2 μm .

Keywords diffusion bonding, mechanical properties, microstructure, pseudo- α -Ti alloy, Ti-stabilized stainless steel

1. Introduction

Stainless steels and titanium alloys are some of the most important structural materials used for manufacturing critical equipment or components used in nuclear, chemical and aerospace industries (Ref 1, 2). Joining stainless steels and titanium alloys using conventional welding technique are challenging because of the significant difference in the thermal expansion coefficient, the limited mutual solubility and the formation of brittle intermetallic compounds. These factors lead to large residual stresses, microstructural inhomogeneity and formation of cracks in the weld. To overcome these problems, different joining methods such as braze welding (Ref 3), diffusion bonding (Ref 1) and explosive bonding (Ref 4) have been investigated to join stainless steels and titanium alloys.

Diffusion bonding is a solid-state welding technique which produces near net shape product and most suitable for joining dissimilar materials. This bonding process involves subsection

of a close contact of materials to be joined to high temperature and pressure (Ref 5). The operating conditions lead to diffusional creep and the inter-diffusion of atoms across the interface resulting in a complete metallurgical bonding (Ref 1, 5). Because of the reactive nature of titanium alloys, bonding of titanium and steels is carried out in vacuum (Ref 1). Many researchers (Ref 2, 6–18) have investigated the diffusion bonding of different kinds of materials using different bonding parameters and interlayers. Their work suggests that the strength of the joint depends on many factors such as the chemical composition of the materials being joined, the microstructural phases present and their distribution prior to the joining and bonding parameters such as temperature, pressure, time, surface preparation and the interlayer used.

Significant volume of research exists on the diffusion bonding of stainless steels and Ti-alloys. Velmurugan et al. (Ref 15) investigated the diffusion bonding of Ti-6Al-4V alloy and duplex stainless steel in the temperature range of 650 to 800 °C for 30 min and reported the presence of intermetallic compounds such as Fe_2Ti , FeTi at the interface and maximum shear strength of 194.3 MPa for the couple bonded at 750 °C. Ghosh et al. (Ref 12) have characterized the CP-Ti and SS304 joint interfaces bonded within a temperature range of 850–950 °C for 60 min, and they reported a maximum tensile strength of ~ 217 MPa for the couple bonded at 850 °C, and at the interface they too found a layer of brittle intermetallic compounds (Fe_2Ti , FeTi and $\text{Fe}_2\text{Ti}_4\text{O}$). Vigraman et al. (Ref 10) investigated the diffusion bond of Ti-6Al-4V and SS 304L in the temperature range of 850–950 °C for 60 min bonding time and found different intermetallic phases such as Fe_2Ti , TiNi_2 , Ti_3Ni_4 , and $\text{Fe}_2\text{Ti}_4\text{O}$, additional Fe_2V_3 , Mn_2Ti , Fe_3Al_2 , Si_4 , Al_6Ti_9 , $\text{Al}_4\text{CrNi}_{15}$ and Ti_2Si_2 phases at the interface and

Harish Kumar, Light Water Reactor Division, Reactor Projects Group, Bhabha Atomic Research Centre, Mumbai 400085, India; **Sujay Bhattacharya**, Reactor Projects Group, Bhabha Atomic Research Centre, Mumbai 400085, India; and **Nachiket A. Keskar**, Mechanical Metallurgy Division, Bhabha Atomic Research Centre, Mumbai 400085, India. Contact e-mail: harishj@barc.gov.in.

also reported maximum tensile strength of 242.6 MPa for the couple bonded at 900 °C. All these investigations revealed that different alloy combinations of the diffusion couple behave differently at particular bonding temperature and time, and therefore, bonding parameters which give maximum strength of the joint are different. These investigations also revealed that brittle intermetallic layer formed at the interface and its width or thickness increases with increasing temperature which consequently resulted in degradation of strength of joint.

To improve the strength of the joint, researchers have also studied stainless steels and Ti alloy diffusion bonding using different interlayers and processing parameters. Sam et al. (Ref 16) studied the diffusion bonding of Ti-6Al-4V and micro-duplex stainless steel using 150- μ m-thick nickel alloy as the interlayer in the temperature range of 800-950 °C for 45 min and reported maximum tensile strength of \sim 560 MPa and a maximum shear strength of \sim 415 MPa for the diffusion couple processed at 900 °C for 45 min. The presence of layers of Ni₃Ti, NiTi and NiTi₂ intermetallics at the nickel alloy/titanium alloy interface was also observed. Similarly, Kundu et al. (Ref 14) studied the diffusion bonding of CP-Ti and SS 304 using 300- μ m-thick pure nickel foil as an interlayer in the temperature range of 800-950 °C and reported a maximum tensile strength of \sim 302 MPa and maximum shear strength of \sim 219 MPa for the diffusion couple processed at 900 °C for 60 min. The layers of Ni₃Ti, NiTi and NiTi₂ were observed at the Ni/Ti interface. The thickness of these intermetallic phases layer was also found to be temperature and time dependent, and larger thickness was detrimental to the strength of the joint. He et al. (Ref 17) investigated the diffusion bonding of Ti-6Al-4V with stainless steel (18Cr10Ni) web using Ni interlayer under different processing parameters and reported optimum bonding temperature of 850 °C, with bonding stress of 10 MPa and time 10-15 min. Similar to others, they also found the presence of intermetallic layers at the Ni-Ti alloy interface. These investigations of stainless steels and Ti alloys diffusion bonding using pure Ni or Ni alloy as interlayer also show different optimum bonding temperature and time for different alloy combinations of the diffusion couple. It is also reported that the brittle Ni-Ti intermetallic layer/s formed at the Ni-Ti alloy interface and the thickness of diffusion zone and intermetallic layer defines the strength of joint.

Thus, it is evident that the formation of layers of brittle intermetallic compounds at diffusion bonded titanium alloys and stainless steels interface is unavoidable, both in the presence and the absence of a Ni-interlayer. However, by adopting a suitable combination of bonding temperature and time, the thickness of this brittle intermetallic layer can be optimized to get maximum joint strength. Also, it can be manifested that couples of different grades of Ti alloy and stainless steels for diffusion bonding with or without Ni interlayer are having different optimum bonding temperature and time, which gives maximum joint strength. However, the extents and the rates of inter-diffusion of atoms during the formation of a diffusion joint depend on the chemical composition and the microstructural phases of the participating alloys (Ref 1). The optimum bonding parameters for couples of different stainless steels and titanium alloys need to be established. There have been many studies of diffusion bonding of α -Ti alloy grades (grades of commercially pure titanium) and commercially available ($\alpha + \beta$)-Ti alloys (Ti-6Al-4V) with different stainless steel grades, available in the literature, but

studies on diffusion bonding between pseudo- α -Ti alloy and stainless steel of grade SS321 are limited.

In the present study, the effect of bonding temperature and time on the thickness of diffusion layer and intermetallic layer was investigated for pseudo- α -Ti alloy and SS321 diffusion joint bonded directly (without interlayer) and with a Ni interlayer. Since diffusion bonding temperature and time for different Ti alloy and stainless steels ranged from 750-950 °C and 1-60 min, respectively; the same range is used in this work. Bonding parameters (bonding temperature and time) which give maximum joint strength in different Ti alloy, and stainless steel diffusion couples were chosen from the literature to shorten the number of experiments, and regimes of bonding parameters were optimized to maximize the resultant shear strength of the joint.

2. Experimental

2.1 Materials

Materials used for the present study are pseudo- α -Ti alloy and Ti-stabilized austenitic stainless steel (SS321). The chemical compositions of the individual alloys used in present investigation are shown in Table 1.

The dimensions of the pseudo- α -Ti alloy and the SS321 samples used in present investigation are shown in Fig. 1. The mating faces of both the samples were ground down to #1200 grit finish and then ultrasonically cleaned in acetone to remove any adhered contaminants.

2.2 Diffusion Bonding

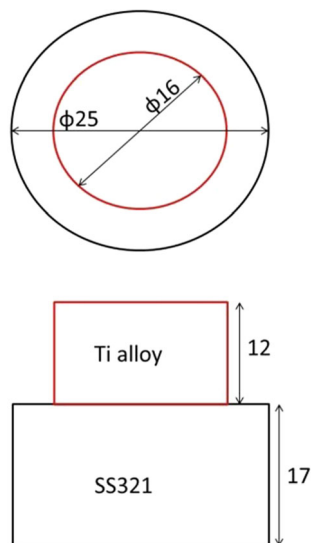
For diffusion bonding of the alloys systems under study was carried out with and without a Ni interlayer. The Ni interlayer was electro-deposited to about \sim 10 μ m thickness on each mating surface of pseudo- α -Ti alloy and SS321. The chemical bath or solution used for the electro-deposition contained nickel sulphate, nickel chloride, tri-sodium citrate and sodium potassium tartrate, and coating was carried out by applying at a current of about 50 mA/cm² using a Santronics ® DC power supply instrument. Diffusion bonding experiments were carried out in an induction-heated vacuum press. The ground (and, in the second case, Ni-coated) mating faces of both the Ti alloy and the SS321 specimens were kept in contact and pre-loaded in induction-heated vacuum press chamber. Before the start of heating, a dynamic vacuum of 4×10^{-4} Pa was attained to avoid oxidation. A constant heating rate of 0.8 °C/s up to 700 °C and 2 °C/s above 700 °C was used for all bonding experiments. After the bonding temperature was achieved, the specimens were loaded to required stress levels.

Initial bonding temperature and time parameters were chosen from literature for different Ti alloy and stainless steels diffusion bonding with maximum joint strength, and further bonding parameters were selected based on the results of initial ones. The matrix of the process parameters used in different bonding experiments is shown in Table 2.

After the end of the bonding cycle, the whole assembly was furnace-cooled under vacuum. After the experiments, joined couples were cut longitudinally across the interface for microstructural investigation of the interface.

Table 1 Chemical composition of Ti alloy and SS321 used in present study. All compositions are in wt.%

| Alloy | C | Fe | Si | Al | V | Cr | Ni | Ti | Mn | O | H | P,S | N |
|----------|------|------|------|-----|-----|------|------|------|------|------|-------|-------|--------|
| Ti alloy | 0.1 | 0.25 | 0.12 | 4.3 | 2.1 | ... | ... | Bal. | ... | 0.15 | 0.006 | ... | 0.04 |
| SS321 | 0.05 | Bal. | 0.35 | ... | ... | 18.5 | 10.5 | 0.45 | 1.45 | ... | ... | <0.02 | <0.015 |

**Fig. 1** Sketch showing the dimensions (in ‘mm’) of the cylindrical samples of pseudo- α -Ti alloy and Ti-stabilized austenitic stainless steel (SS321), used for bonding experiments in present investigation**Table 2 Bonding process parameters used in the pseudo- α -Ti alloy and SS321 diffusion bonding experiments**

| | Bonding temperature, °C | Bonding load, kN | Bonding time, min |
|----------------------|-------------------------|------------------|-------------------|
| Without inter-layer | 800 | 13.6 | 45, 60 |
| | 900 | 4.8 | 45, 60 |
| | 920 | 4.8 | 8, 15, 25, 45 |
| With ‘Ni’ interlayer | 800 | 13.6 | 15 |
| | 850 | 10.4 | 15 |
| | 900 | 4.8 | 35, 45 |
| | 920 | 4.5 | 35, 45 |
| | 940 | 4 | 1 |

2.3 Microstructural Characterization

The samples for microstructural analysis were mechanically ground down to 2400 grit finish and then further polished using diamond suspension up to 3 μm finish. The polished samples were then etched with a solution of 5ml HF, 40 ml HNO_3 and 55 ml H_2O . Etched samples were then examined using a Carl Zeiss® optical microscope and a Carl Zeiss® Field Emission-Scanning Electron Microscope (FESEM). The compositional analysis of the interface was carried out using an Oxford Instruments® energy-dispersive x-ray spectroscopy attached to the FESEM.

2.4 Mechanical Testing

Hardness measurement across the joint interface was carried out on LECO® micro-hardness tester using a 50 g force for a dwell time of 15 s.

Figure 2(b) shows the design of shear testing setup used in present investigation. Shear testing was carried out to determine the shear strength of the bonded joint at room temperature using a 100 kN capacity Zwick Roell® screw driven universal testing machine. The shear test specimens with dimensions of 5 mm \times 5 mm \times 29 mm as shown in Fig. 2(a) were machined from the bonded diffusion couple. A minimum of three tests for each bonding conditions were carried out to determine the statistical scatter in resulting shear strength and ensure repeatability. A crosshead speed of 0.2 mm/min was used for all tests.

3. Results

In the present study, parametric studies on the diffusion bonding of SS321 and Ti-alloy were carried out. The parameters evaluated were the diffusion bonding temperature, the bonding time and the interlayer. The effects of these parameters on the shear strength of the diffusion bonded joint are detailed in the following paragraphs. The results are divided into three sections: (a) microstructure of the interfacial region, (b) kinetics of the growth of the interfacial region and (c) the mechanical properties of the diffusion bonded joints.

3.1 Microstructure of the Interfacial Region

The microstructures of the starting materials (SS321 and the Ti-alloy) are shown in Fig. 3.

It may be noted that both the alloys were in a fully recrystallized condition, with equiaxed grains. The average grain size of the SS321 was $\sim 30 \mu\text{m}$, while that of the Ti-alloy was $\sim 20 \mu\text{m}$ determined using line-intercept method. After direct diffusion bonding of these constituent alloys, in the temperature range of 800 to 920 °C for different time durations as given in Table 2, the microstructure of the diffusion zone was seen to be composed of three different reaction layers: (i) layer of intermetallic compounds, (ii) layer of transformed β -Ti phase and (iii) layer of mixed α + β -Ti-phases. Figure 4 presents the FESEM micrographs showing interface microstructure of the diffusion couples bonded at temperature ranges from 800 to 920 °C for 45 min.

The EDS line profile shown in Fig. 5 shows the variation in the composition across the diffusion zone for the couple diffusion bonded at 900 °C for 45 min. The layer of intermetallic compounds consisted of a Cr-rich layer toward the SS321 side, and adjacent to this, a layer of Fe-Ti intermetallic compounds was found. Composition analysis using EDS indicates the presence of presumably Fe_2Ti and FeTi intermetallic compounds in the intermetallic layer at the interface.

This layer was followed by a layer of gradually decreasing Fe-content, from SS 321 side to the Ti-alloy side and having Fe greater than ~9.2 wt.%. At the end of this layer, a layer of mixed $\alpha + \beta$ -Ti-phases with Fe less than ~9 wt.%, with a typical basket-weave structure, was observed.

In the case of the diffusion bonding of the SS 321-Ti alloy *in the presence of a Ni interlayer*, an interfacial region composed of two diffusion zones was observed: (a) the SS 321-Ni interface and (b) the Ni-Ti alloy interface. Figure 6 presents the FESEM micrographs showing the microstructure of interface across the diffusion couples bonded using Ni interlayer at different bonding temperatures for different time intervals. The SS-Ni interface was diffuse, with no intermetallic compounds.

As seen in the EDS profile in Fig. 7, it was observed that, across SS321-Ni interface, composition changes gradually for Ni, Cr and Fe. Going from the SS321 side to the Ni side, the variations in the Cr, Fe and Ni contents were 5 to 2.5, 18 to 5.5 and 20 to 43 in atomic %, respectively. The Ni-Ti alloy interface was composed of two distinct layers: (a) layer of intermetallic compounds and (b) layer of ($\alpha + \beta$)-Ti-phases. The EDS analysis of the layer of intermetallic compounds, as shown in Fig. 8, showed the presence of sub-layers of three distinct compositions.

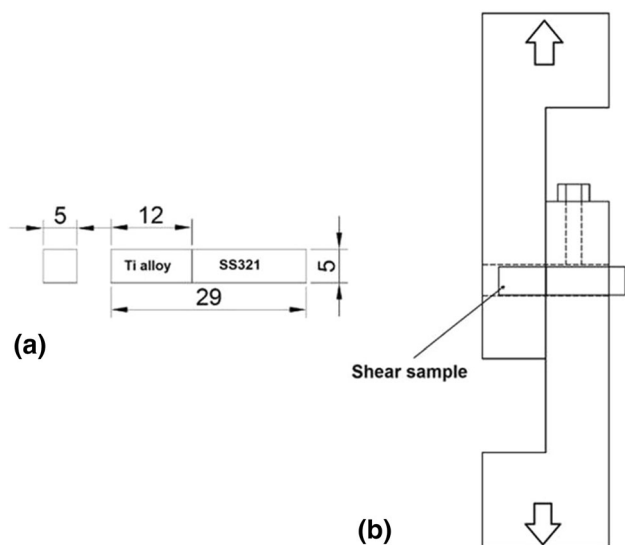


Fig. 2 Sketch of (a) shear test specimen (dimensions in 'mm'), (b) shear test setup

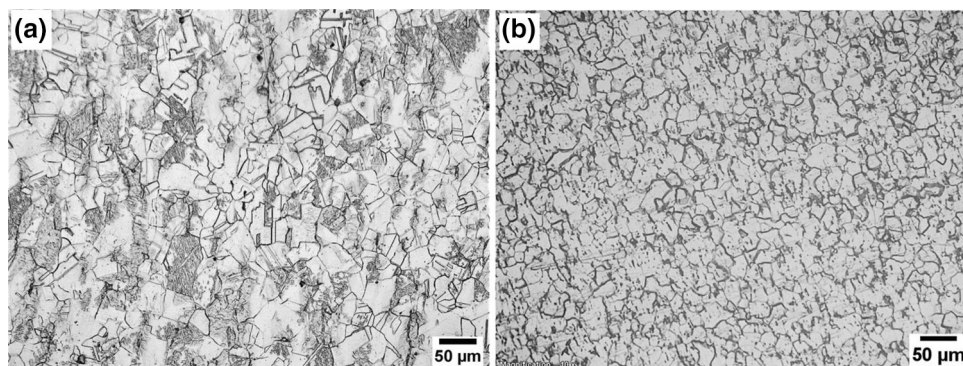


Fig. 3 Optical micrographs of as-received (a) SS321 and (b) pseudo- α -Ti alloy

The sub-layer adjacent to Ti alloy side, marked by point C in Fig. 8, had a composition of Ti (~60 at.%), Ni (~29 at.%) and Al (~9 at.%) with small amounts of V (~1.6 at.%) and Fe (~0.2 at.%). The phase diagram of Ti and Ni indicates that the layer is presumably the NiTi₂ phase (Ref 20). The layer closer to the Ni side, marked by point A in Fig. 8, was found to be enriched with Ti (~22 at.%), Ni (~75 wt.%), Al (~3 at.%), V (~0.3 at.%), which indicated the possible Ni₃Ti phase (Ref 20). In between Ni₃Ti phase and Ti₂Ni phase, another layer of TiNi, marked with point B in Fig. 8, was observed. This layer was enriched with Ti (~46 at.%), Ni (~49 at.%), Al (~5 at.%) and V (~0.3 at.%) (Ref 20). The layer of $\alpha + \beta$ Ti phases was microstructurally distinguishable due to the presence of a basket-weave structure.

3.2 Kinetics of the Growth of the Interfacial Region

The details of the thicknesses of various layers of the diffusion zone are listed in Table 3. Overall, the thickness of the diffusion zone was observed to increase with the increase in the bonding temperature as well as the bonding time. The layer of intermetallic compounds was the slowest growing layer in all the samples. The maximum diffusion zone of ~125 μm and ~54 μm was obtained with and without the Ni-interlayer, respectively, in the diffusion couples bonded at 920 °C for 45 min. According to diffusion reaction kinetics, time dependent growth of the diffusion reaction layers can be expressed as follows (Ref 2, 18, 19).

$$x = Bt^{1/2} \quad (\text{Eq 1})$$

where x is the thickness or width of the reaction layer (m), t is the bonding time (s) and B is the rate constant of diffusion reaction ($\text{m/s}^{1/2}$).

The temperature dependence of growth of the diffusion layers follows the Arrhenius equation and can be represented by the following equation in conjunction with Eq. 1 (Ref 2, 16).

$$x = B_0 \exp\left(-\frac{Q}{RT}\right) t^{1/2} \quad (\text{Eq 2})$$

where Q is the activation energy (kJ/mol), B_0 is the rate constant ($\text{m/s}^{1/2}$), R is the real gas constant (8.314 J/mol/K) and T is the bonding temperature (K).

Figure 9 shows the plot of x versus $t^{1/2}$ for diffusion zone, intermetallic layer and transformed β -Ti phase layer for the direct bonded diffusion couples, bonded at 920 °C for different bonding time. The average rate constant (slope of the x versus

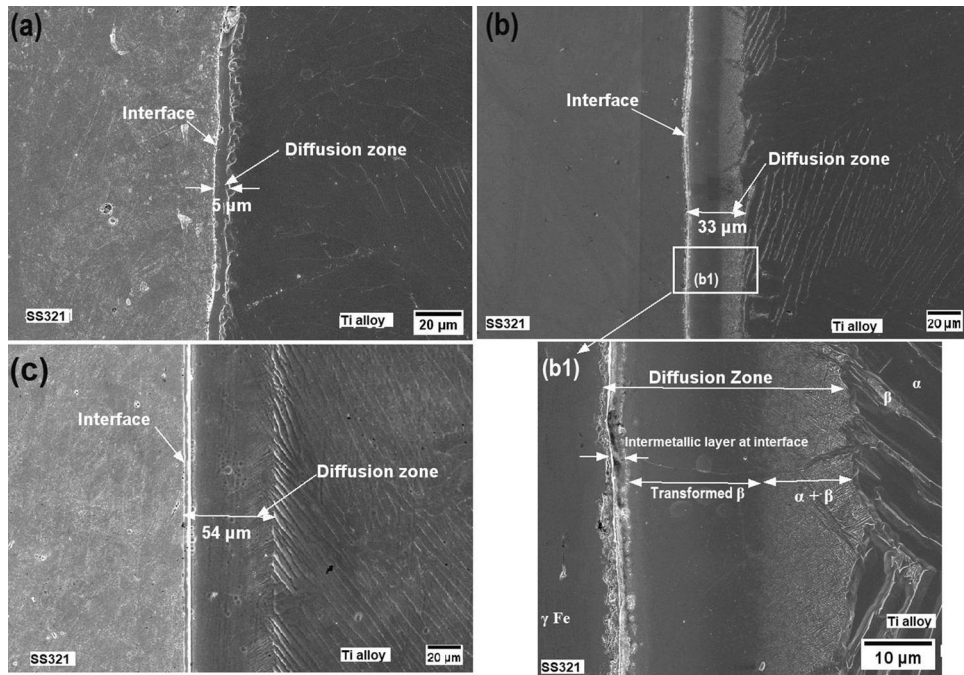


Fig. 4 SEM micrographs of interface of the SS321-Ti alloy couples diffusion bonded at temperature (a) 800 °C, (b) 900 °C and (c) 920 °C, for 45 min. (b1) is the higher magnification image of selected region of (b) showing different layers present at the joint interface

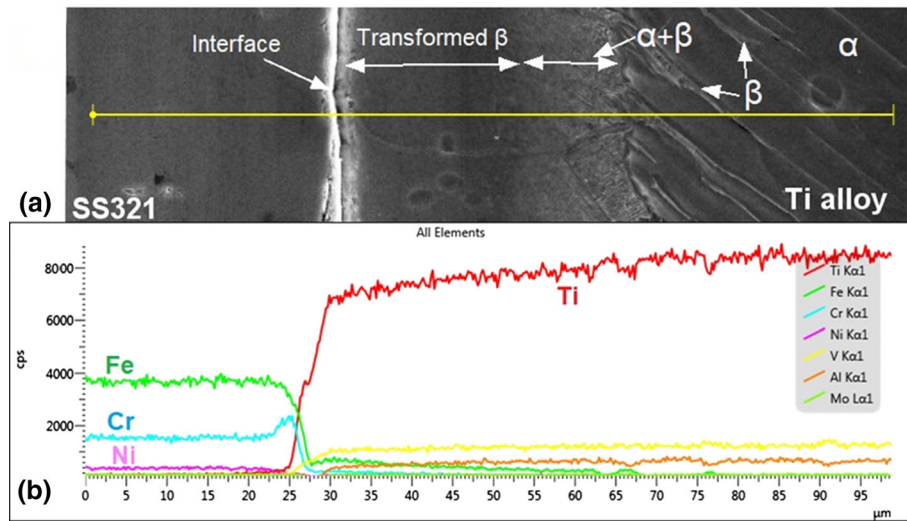


Fig. 5 EDS elemental concentration profile across the SS321-Ti alloy interface of the couple bonded at 900 °C for 45 min: (a) SEM image showing the line across the interface, (b) line scanning concentration profiles

$t^{1/2}$) for the diffusion zone was $1.32 \times 10^{-6} \text{ m/s}^{1/2}$ while that for the intermetallic layer and transformed β -Ti phase layer was $1.14 \times 10^{-7} \text{ m/s}^{1/2}$ and $7.04 \times 10^{-6} \text{ m/s}^{1/2}$. The value of the activation energy (Q) was obtained from the slope of the linear fitting of $\ln(x)$ versus $1/T$ for all the layers as per Eq. 2, while the intercept yields the value of rate constant (B_0) for the particular diffusion layer. Table 4 presents the values of Q and B_0 for different diffusion/reaction layers for the direct bonded diffusion couples, bonded at different bonding temperature for

45 min. The value of Q was seen to be the lowest for the transformed β layer and the highest for the $\alpha + \beta$ layer.

3.3 The Mechanical Properties of the Diffusion Bonded Joints

In all the diffusion bonded joints, the diffusion zone was seen to be harder than both the constituent alloys. A representative case of the joint, diffusion bonded at 900 °C

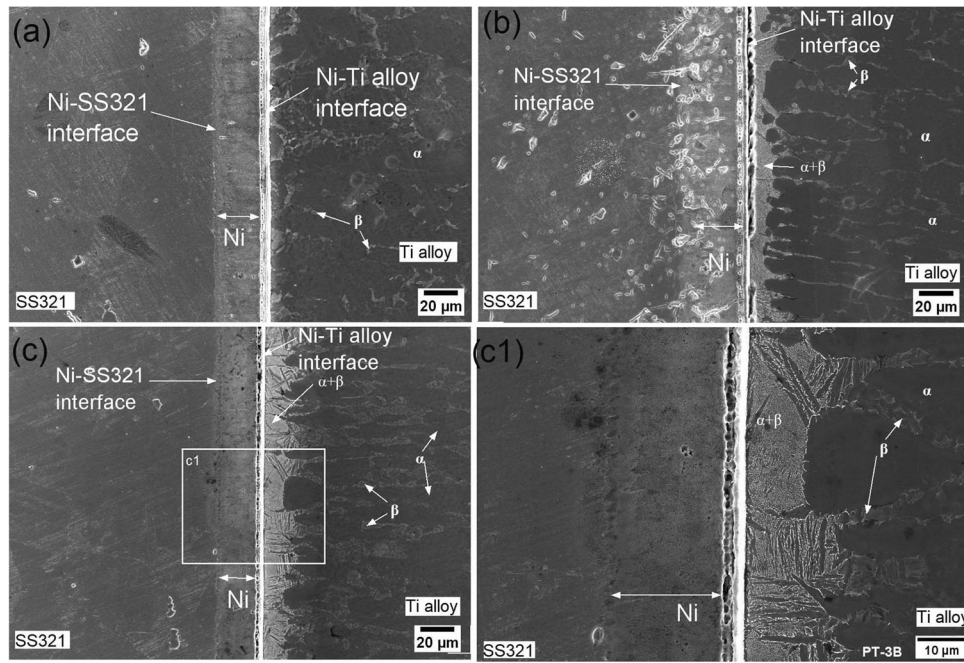


Fig. 6 SEM micrographs of interface of the SS321-Ti alloy couples diffusion bonded (with Ni interlayer) at bonding temperature (a) 800 °C (b) 850 °C and (c) 940 °C, for 15, 15 and 1 min, respectively. (c1) is the higher magnification image of selected region of (c) showing different layers present at the bonding interface

for 45 min, directly and with Ni interlayer, is shown in Fig. 10(a) and (b), which shows the micro-hardness variation across the joint interface. The hardness of the interface was seen to increase with the increase in the thickness of the intermetallic layer as shown representatively in Fig. 11.

Shear testing of the diffusion bond for the couples bonded directly, and with Ni interlayer at different processing conditions, was carried out at room temperature. Table 5 shows the average shear strength of the joint bonded directly and with Ni interlayer at different temperatures and time. Figure 12 shows the variation in the shear strength with thickness of diffusion zone and intermetallic layer for diffusion couples bonded directly and with Ni interlayer.

It was observed that shear strength of the diffusion couples increased monotonically with the thickness of the diffusion zone, up to a thickness of $\sim 20 \mu\text{m}$ and $\sim 14 \mu\text{m}$ for joints with interlayer and directly bonded, respectively. However, a further increase in the thickness of the diffusion zone coincided with a decrease in the shear strength. The maximum shear strength of $223 \pm 17 \text{ MPa}$ was observed in the couple direct diffusion bonded at 920 °C bonding temperature for 8 min, with a diffusion zone thickness of $\sim 14 \mu\text{m}$ and a $\sim 1.5\text{-}\mu\text{m}$ -thick intermetallic layer.

4. Discussion

The present work was aimed at optimizing the diffusion bonding parameters of SS321 and pseudo- α -Ti alloy couple on the basis of maximization of the shear strength of the diffusion bond. The shear strength of the diffusion bonded couples is a

function of the diffusion zone as well as the thickness of the intermetallic zones. The thickness of the diffusion zone and the intermetallic zone generally increased with the increase in temperature (though at different rates) and bonding time, as expected. However, the variation in the shear strength was non-monotonic with the increase in the thickness of the diffusion zone or the intermetallic zone. Thus, the shear strength is the result of the interplay of the effects of various layers that constituted the diffusion zone. The following paragraphs discuss the roles that various layers of the diffusion zone play, in the determination of the shear strength of the diffusion bond.

The transformed β layer was the fastest growing layer in the diffusion zone of the direct bonded diffusion couples. Across the interface, it was found that Fe atoms diffuse in Ti alloy to a larger distance compared to diffusion of Ti atoms in SS321 side. Since Fe is a stabilizer of β -Ti phase, it can be inferred that the fast diffusion of Fe in Ti alloy was responsible for the formation of the layer of transformed β -Ti phase at an enhanced rate. Further, the Cr-rich layer observed close to the SS321 (see Fig. 5a) side can be attributed to an apparent uphill diffusion of Cr. It is known that the diffusion of Ti in SS321 decreases the activity of Cr (Ref 11). Thus, the diffusion of Cr appears to have occurred down the activity gradient, instead of the concentration gradient.

In the case of the diffusion couples with Ni interlayer, no intermetallic compounds were formed in the Ni-SS321 side, owing to the significant solubility of Ni in Fe. On the other hand, at the Ni-Ti alloy interface, a distinct intermetallic layer was found. From Ni-Ti phase diagram (Ref 20), it can be seen that several line compounds are possible. Hence, several sub-layers of varying proportions of Ni and Ti were found within the intermetallic layer. Ni is known to stabilize the β -phase in

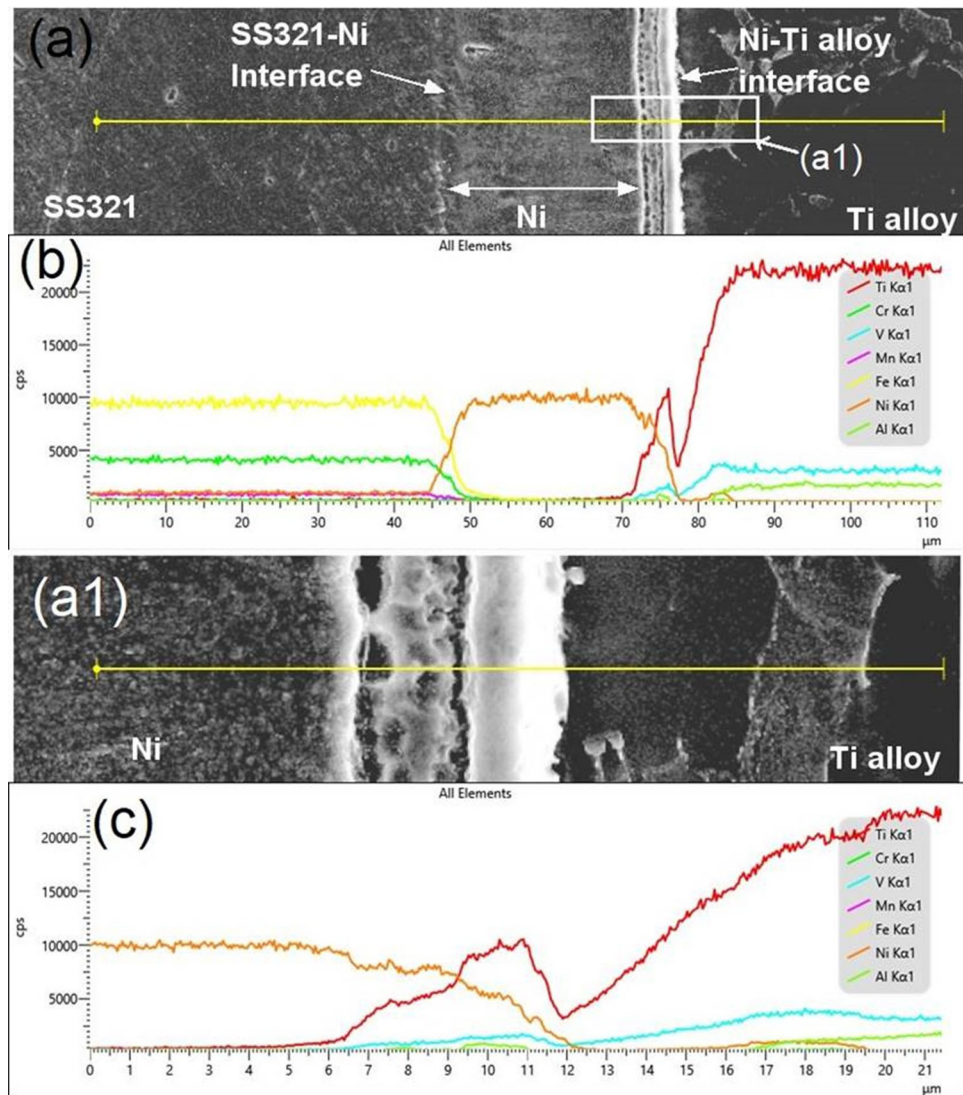


Fig. 7 EDS elemental concentration profile across the SS321-Ni-Ti alloy interface of the couple bonded with Ni interlayer at 850 °C for 15 min (a) SEM image showing the line across the SS321-Ni-Ti alloy interface (b) line scanning concentration profiles across the interface

Ti, and hence, the diffusion of Ni into Ti could have transformed the α -Ti to β -Ti (Ref 22). Further away from the Ni interlayer and into the Ti side, decreasing Ni content is expected to have destabilized the β -Ti phase upon cooling and resulted in the Widmanstätten type $\alpha+\beta$ layer (Ref 14).

There is the migration of the bonding interfaces in the third stage of diffusion bonding, following the deformation of micro-asperities (first stage) and shrinking of interface voids via creep and diffusion-controlled mass transport (second stage) (Ref 23). Greater extent of diffusion of elements across the interface (a wider diffusion zone) generally results in a void free diffusion joint with a good joint strength. It is evident from the current

study and the literature (Ref 1, 8, 10, 12) that the strength of the diffusion bond is a function of the thickness of diffusion zone and intermetallic layer. However, this function is not monotonic. Although the application of higher bonding temperature and longer bonding time leads to a wider diffusion zone, it also widens the intermetallic layer present at the interface (Ref 12). This intermetallic layer is composed of different brittle intermetallic compounds which can be detrimental to the strength of the joint (Ref 1). Thus, in the present study, while an initial increment in the bonding temperature and / or time resulted in the increase in the shear strength of the joint due to enhanced diffusion, extended increments in either of these

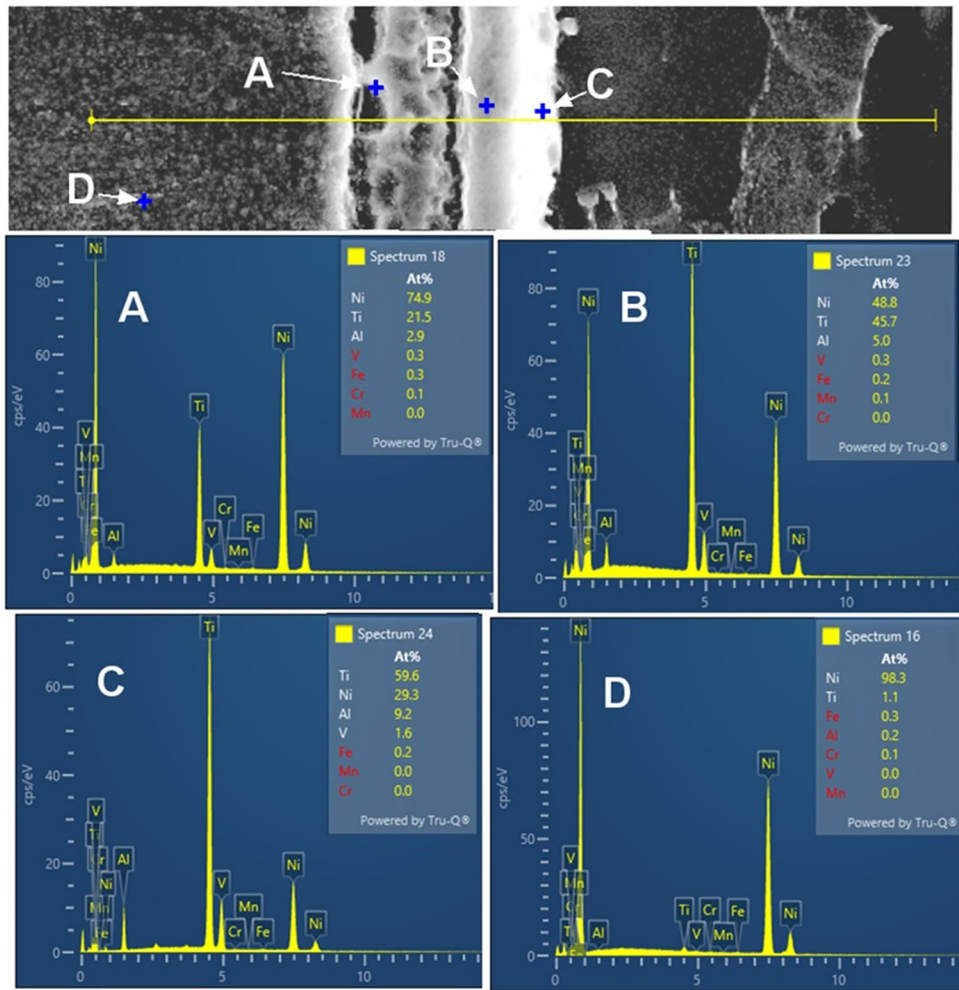


Fig. 8 EDS analysis showing the composition of sub layers present at the Ni-Ti alloy interface; points A, B and C present the sub-layers of Ni_3Ti , NiTi, NiTi_2 phases, respectively. Point D represents Ni layer

parameters (temperature and time) resulted in the formation of a thicker brittle intermetallic layer, which evidently, weakened the joint.

That is why, for direct diffusion bonded couples, maximum shear strength (223 ± 17 MPa) was observed for the diffusion couple (920°C for 8 min) with ~ 1.5 and ~ 14 μm thickness of intermetallic layer and diffusion zone, respectively. In contrast, the diffusion bonded couple (920°C for 15 min) with a wider diffusion zone (~ 18 μm) and a wider intermetallic layer (~ 1.8 μm) had lower shear strength of 183 ± 3 MPa. Further reduction in the thickness of the intermetallic layer is accompanied by an insufficient thickness of the diffusion zone, resulting in reduced strength. Similar results were observed for the diffusion couples with Ni interlayer, wherein the maximum shear strength (180 ± 23 MPa) was obtained for the couple (940°C for 1 min) with ~ 4 - μm intermetallic layer and the lowest strength was seen in the couple with a 29 μm

intermetallic layer. Therefore, the bonding temperature and bonding time need to be optimized in such a way as to minimize the thickness of intermetallic layer for a particular thickness of the diffusion zone.

5. Summary and Conclusions

The diffusion bonding of pseudo- α -Ti alloy and Ti-stabilized stainless steel (SS321), with and without interlayer, at different bonding temperatures and time was studied to determine the optimum bonding process parameters and thickness of intermetallic and diffusion zone layers. The conclusions derived from the present study are as follows:

1. Diffusion zone composed of three different layers (i) Fe-Ti intermetallic phase layer, (ii) transformed β layer and

Table 3 Thicknesses of the diffusion zones and the intermetallic layers of the diffusion couples bonded directly (without interlayer), and with Ni interlayer at different processing parameters

| Without interlayer | | | | | | | | | | With Ni interlayer | | | |
|-------------------------|-------------------|---------------------------------|--------------------------------------|--|-----------------------------------|--|-------------------------|-------------------|----------------------------------|--|---|--|--|
| Bonding temperature, °C | Bonding time, min | Thickness of diffusion zone, μm | Thickness of intermetallic layer, μm | Thickness of Fe-Ti intermetallic layer, μm | Thickness of β-Ti phase layer, μm | Thickness of (α + β) -Ti phase layer, μm | Bonding temperature, °C | Bonding time, min | Thickness of diffusion zone*, μm | Thickness of intermetallic phase layer**, μm | Thickness of (α + β) - Ti phase layer, μm | | |
| 800 | 45 | ~5 | ~0.5 | ~4 | ~0.5 | ~0.5 | 800 | 15 | ~7 | ~5.5 | ~1.5 | | |
| 800 | 60 | ~9 | ~0.75 | ~7 | ~1 | ~1 | 850 | 15 | ~17 | ~7 | ~10 | | |
| 900 | 45 | ~33 | ~2 | ~17 | ~14 | ~14 | 900 | 35 | ~70 | ~10 | ~60 | | |
| 900 | 60 | ~45 | ~4 | ~25 | ~16 | ~16 | 900 | 45 | ~73 | ~11 | ~62 | | |
| 920 | 8 | ~14 | ~1.5 | ~8 | ~4 | ~4 | 920 | 35 | ~103 | ~22 | ~81 | | |
| 920 | 15 | ~18 | ~1.8 | ~10 | ~6 | ~6 | 920 | 45 | ~125 | ~29 | ~96 | | |
| 920 | 25 | ~23 | ~1.9 | ~14 | ~7 | ~7 | 940 | 1 | ~20 | ~4 | ~16 | | |
| 920 | 45 | ~54 | ~5 | ~29 | ~20 | ~20 | | | | | | | |

*Diffusion zone is the average total thickness of (α+β) phase and Ni-Ti intermetallic layer. ** Composed of Ni₃Ti, NiTi, NiTi₂

- (iii) $\alpha+\beta$ phase layer was observed in the directly bonded diffusion joint. Thickness of these reaction layers increased with increasing temperature and time, and determined the strength of the diffusion joint.
- For direct diffusion bonding, the maximum shear strength of the joint was found in the diffusion couple bonded at 920 °C for 8 min and having an intermetallic layer of $\sim 1.5 \mu\text{m}$, and a diffusion zone of $\sim 14 \mu\text{m}$. From all the tested bonding parameters, it can be expected that optimum bonding temperature regime to be 900-920 C for bonding time of 8-30 min for maximum shear strength. These process parameters can be ex-

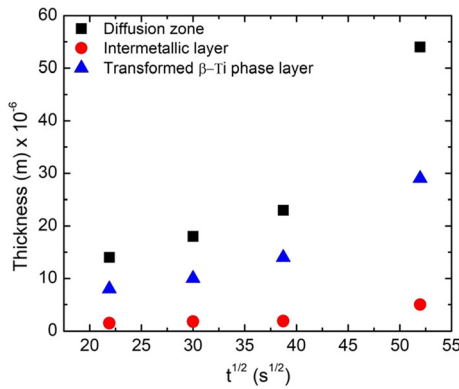


Fig. 9 Plot of x vs. $t^{1/2}$ for diffusion zone, intermetallic layer and transformed β -Ti phase layer

- pected to produce an intermetallic layer of $\sim 2 \pm 0.5 \mu\text{m}$ and a diffusion zone of greater than $14 \mu\text{m}$.
- For diffusion bonding using Ni as an interlayer, layerwise Ni_3Ti , NiTi and Ti_2Ni intermetallic compounds have been observed at Ni-Ti alloy interface, and their thickness increases with increase in bonding temperature.
 - The maximum shear strength of the joint with Ni interlayer was found in the diffusion couple bonded at 940 °C for 1 min and having an intermetallic layer of $\sim 4 \mu\text{m}$ and a diffusion zone of $\sim 20 \mu\text{m}$.

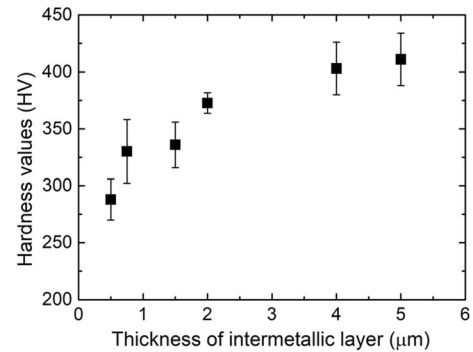


Fig. 11 Variation in bond interface hardness with thickness of intermetallic layer for direct bonded diffusion couples

Table 4 Layer growth kinetics of the diffusion/reaction layers formed in the SS321-Ti alloy interface.

| Diffusion/reaction layers | Activation energy (Q), kJ/mol | Growth constant (B_0), $\text{m/s}^{1/2}$ |
|---------------------------|-----------------------------------|---|
| Diffusion zone | 202 | 2.06×10^1 |
| Intermetallic layer | 180 | 1.6×10^{-1} |
| Transformed β layer | 164 | 2.1×10^{-1} |
| $(\alpha+\beta)$ Ti layer | 327 | 3.6×10^6 |

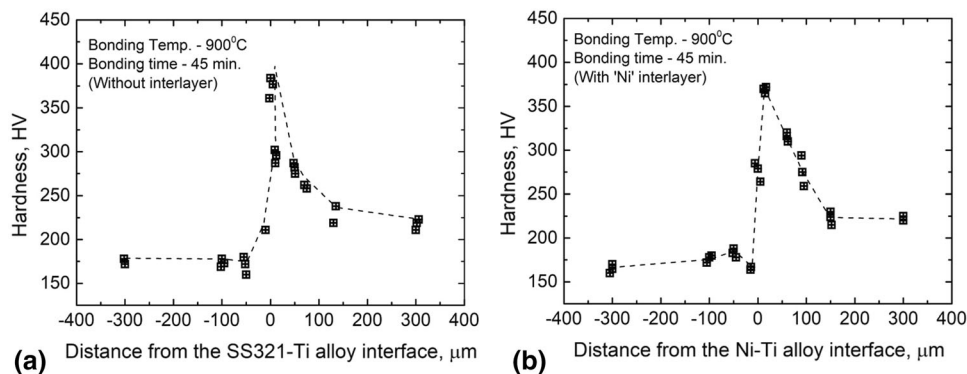


Fig. 10 Hardness variation across the interface of samples (a) directly (without interlayer) bonded at 900 °C for 45 min and (b) bonded at 900 °C for 45 min with 'Ni' interlayer. Dotted line shows trend of hardness across the interface.

Table 5 Shear strength of the diffusion couples bonded directly (without interlayer) and with Ni interlayer at different processing parameters

| Without interlayer | | | | | With Ni interlayer | | | | |
|-------------------------|-------------------|--|---|-----------------------------|-------------------------|--------------------|--|---|-----------------------------|
| Bonding temperature, °C | Bonding time, min | Thickness of diffusion zone, μm | Thickness of Fe-Ti intermetallic phase layer, μm | Average shear strength, MPa | Bonding temperature, °C | Bonding time, min) | Thickness of diffusion zone, μm | Thickness of Ni-Ti intermetallic phase layer, μm | Average shear strength, MPa |
| 800 | 45 | ~5 | ~0.5 | 93 \pm 19 | 800 | 15 | ~7 | ~5.5 | 71 \pm 12 |
| 800 | 60 | ~9 | ~0.75 | 155 \pm 22 | 850 | 15 | ~17 | ~7 | 164 \pm 18 |
| 900 | 45 | ~33 | ~2 | 162 \pm 11 | 900 | 35 | ~70 | ~10 | 77 \pm 28 |
| 900 | 60 | ~45 | ~4 | 154 \pm 11 | 900 | 45 | ~73 | ~11 | 89 \pm 17 |
| 920 | 8 | ~14 | ~1.5 | 223 \pm 17 | 920 | 35 | ~103 | ~22 | 98 \pm 8 |
| 920 | 15 | ~18 | ~1.8 | 183 \pm 3 | 920 | 45 | ~125 | ~29 | 34 \pm 3 |
| 920 | 25 | ~23 | ~1.9 | 182 \pm 13 | 940 | 01 | ~20 | ~4 | 180 \pm 23 |
| 920 | 45 | ~54 | ~5 | 131 \pm 23 | | | | | |

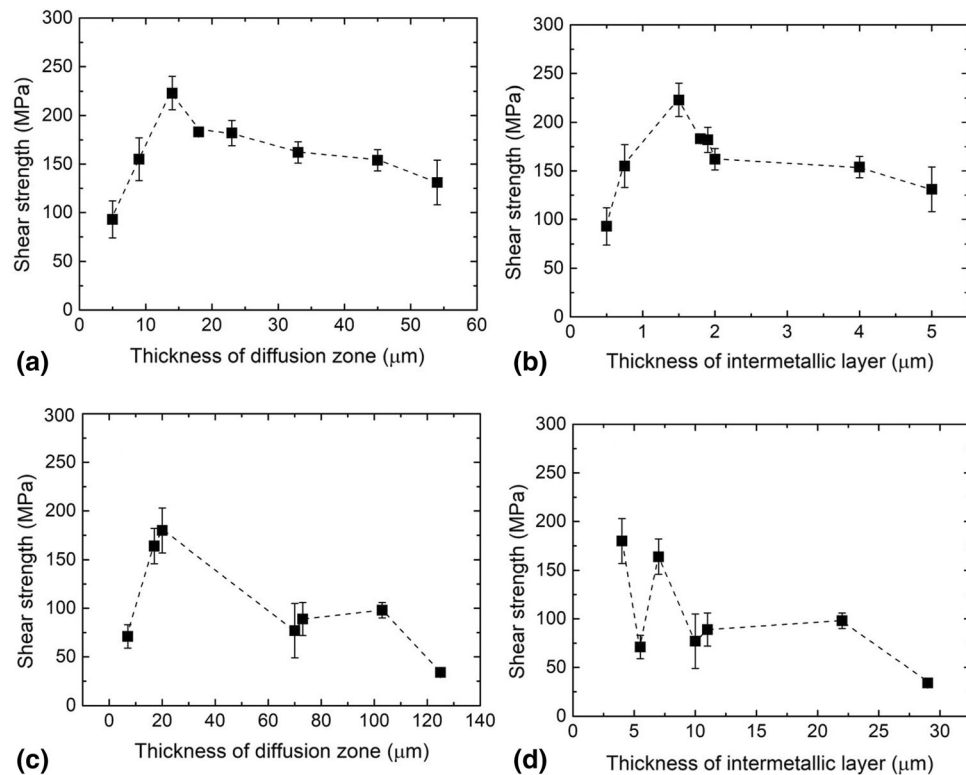


Fig. 12 Shear strength vs. thickness of diffusion layer and intermetallic layer of couples, (a) and (b) directly bonded (without interlayer) and (c) and (d) bonded with Ni interlayer

Acknowledgments

The authors would like to acknowledge Dr. S. K Ghosh, SO/H, Dr R. N Singh, Head, Mechanical Metallurgy Division Dr. V. Kain, Director Materials Group of Materials group and Head CDM, BARC, for providing the laboratory facilities during the investigation. The author would also like to acknowledge Shri B.K Mishra for provided all the logistical help for carrying out the experiments and Shri Bhupendra Kumawat for helping to carry out shear testing.

References

1. D. Mo, T. Song, Y. Fang, X. Jiang, C.Q. Luo, M.D. Simpson and Z. Luo, A Review on Diffusion Bonding between Titanium Alloys and Stainless Steels, *Adv. Mater. Sci. Eng.*, 2018, **2018**, p 8701.
2. G.B. Kale, R.V. Patil and P.S. Gawade, Interdiffusion Studies in Titanium-304 Stainless Steel System, *J. Nucl. Mater.*, 1998, **257**, p 44–50.
3. Y. Xia, P. Li, X. Hao and H. Dong, Interfacial Microstructure and Mechanical Property of TC4 Titanium alloy/316L Stainless Steel Joint Brazed with Ti-Zr-Cu-Ni-V Amorphous Filler Metal, *J. Manuf. Process.*, 2018, **35**, p 382–395.

4. Q. Zhou, R. Liu, Q. ZHOU, P. Chen and L. Zhu, Microstructure Characterization and Tensile Shear Failure mechanism of the Bonding Interface of Explosively Welded Titanium-Steel Composite, *Mater. Sci. Eng. A.*, 2021, **820**, p 141559.
5. N.F. Kazakov, *Diffusion Bonding of Materials*, 1st ed. Mir Publishers, Moscow, 1985
6. S. Li, D. Du, Y. Jiu, J. Qin, Q. Liu and W. Long, Brazing of C/C Composite and TiAl Alloy Using TiNiSi Filler Metal Added Cu Interlayer, *J. Mater. Eng. Perform.*, 2021 <https://doi.org/10.1007/s11665-021-06251-9>
7. C. Liu, C. Mao, L. Cui, X. Zhou, L. Yu and Y. Liu, Recent Progress in Microstructural Control and Solid-State Welding of Reduced Activation Ferritic/Martensitic Steels, *Acta Metall. Sin.*, 2021, **57**(11), p 1521–1538.
8. J. Xiong, Y. Peng, M. Samiuddin, L. Yuan and J. Li, Common Mechanical Properties of Diffusion Bonded Joints and Their Corresponding Microstructure Features, *J. Mater. Eng. Perform.*, 2020, **29**, p 3277–3286.
9. B. Aleman, L. Gutierrez and J.J. Urcola, Interface Microstructures in Diffusion Bonding of Titanium Alloys to Stainless and Low Alloy Steels, *Mater. Sci. Technol.*, 1993, **9**, p 633.
10. T. Vigraman, D. Ravindran and R. Narayanasamy, Effect of Phase Transformation and Intermetallic Compounds on the Microstructure and Tensile Strength Properties of Diffusion-Bonded Joints Between Ti-6Al-4V and AISI 304L, *Mater. Des.*, 2012, **36**, p 714–727.
11. K. Bhanumurthy and G.B. Kale, Reactive Diffusion Between Titanium and Stainless Steel, *J. Mater. Sci. Lett.*, 1993, **12**, p 1879–1881.
12. M. Ghosh and S. Chatterjee, Characterization of Transition Joints of Commercially Pure Titanium to 304 Stainless Steel, *Mater. Charact.*, 2002, **48**, p 393–399.
13. A. Elrefaey and W. Tillmann, Solid State Diffusion Bonding of Titanium to Steel Using a Copper Base Alloy as Interlayer, *J. Mater. Process. Technol.*, 2009, **209**, p 2746–2752.
14. S. Kundu and S. Chatterjee, Interfacial Microstructure and Mechanical Properties of Diffusion-Bonded Titanium–Stainless Steel Joints Using a Nickel Interlayer, *Mater. Sci. Eng. A.*, 2006, **425**, p 107–113.
15. C. Velmurugan, V. Senthilkumar, S. Sarala and J. Arivarasan, Low Temperature Diffusion Bonding of Ti-6Al-4V and Duplex Stainless Steel, *J. Mater. Process. Technol.*, 2016, **234**, p 272–279.
16. S. Sam, S. Kundu and S. Chatterjee, Diffusion Bonding of Titanium Alloy to Micro-duplex Stainless Steel Using a Nickel Alloy Interlayer: Interface Microstructure and Strength Properties, *Mater. Des.*, 2012, **40**, p 237–244.
17. P. He, J. Zhang, R. Zhou and X. Li, Diffusion Bonding Technology of a Titanium Alloy to a Stainless Steel Web With an Ni Interlayer, *Mater. Charact.*, 1999, **43**, p 287–292.
18. T.F. Song, X.S. Jiang, Z.Y. Shao, Y.J. Fang, D.F. Mo, D.G. Zhu and M.H. Zhu, Microstructure and Mechanical Properties of Vacuum Diffusion Bonded Joints Between Ti-6Al-4V Titanium Alloy and AISI316L Stainless Steel Using Cu/Nb Multi-interlayer, *Vacuum*, 2017, **145**, p 68–76.
19. S. Taktak and H. Akbulut, Diffusion Kinetics of Explosively Treated and Plasma Nitride Ti-6Al-4V Alloy, *Vacuum*, 2004, **75**, p 247–259.
20. T.B. Massalski and H. Okamoto, *Binary Alloy Phase Diagrams*, 2nd ed. ASM International, Materials Park, 1990
21. P. Novak, V. Vojtich, Z. Pecanova, F. Prua, P. Pokorny, D. Deduytsche, C. Detavernier, A. Bernatikova, P. Salvetr, A. Knaislova, K. Nova and L. Jaworska, Formation of Ni-Ti Intermetallics During Reactive Sintering at 800–900 °C, *Mater. technol.*, 2017, **51**, p 679–685.
22. C. Leyens and M. Peters, *Titanium and Titanium Alloys—Fundamentals and Applications*, WILEY-VCH Verlag GmbH & Co. KGaA, Weinheim, 2003
23. M.W. Mahoney and C.C. Bampton, Fundamentals of Diffusion Bonding, *Welding, Brazing, And Soldering*, Vol 6, 10th ed., D.L. Olson et al., Ed., ASM International, Materials Park, 1993

Publisher's Note Springer Nature remains neutral with regard to jurisdictional claims in published maps and institutional affiliations.